

Accepted Article

Title: Steering Surface Reaction Dynamics with Self-Assembly Strategy

Authors: Xiong Zhou, Chenguang Wang, Yajie Zhang, Fang Cheng, Yang He, Qian Shen, Jian Shang, Xiang Shao, Wei Ji, Wei Chen, Guoqin Xu, and Kai Wu

This manuscript has been accepted after peer review and appears as an Accepted Article online prior to editing, proofing, and formal publication of the final Version of Record (VoR). This work is currently citable by using the Digital Object Identifier (DOI) given below. The VoR will be published online in Early View as soon as possible and may be different to this Accepted Article as a result of editing. Readers should obtain the VoR from the journal website shown below when it is published to ensure accuracy of information. The authors are responsible for the content of this Accepted Article.

To be cited as: *Angew. Chem. Int. Ed.* 10.1002/anie.201705018
Angew. Chem. 10.1002/ange.201705018

Link to VoR: <http://dx.doi.org/10.1002/anie.201705018>
<http://dx.doi.org/10.1002/ange.201705018>

COMMUNICATION

Steering Surface Reaction Dynamics with Self-Assembly Strategy

Xiong Zhou, Chenguang Wang, Yajie Zhang, Fang Cheng, Yang He, Qian Shen, Jian Shang, Xiang Shao,* Wei Ji,* Wei Chen, Guoqin Xu, Kai Wu*

Abstract: Ullmann coupling of 4-bromobiphenyl by thermally catalyzed on Ag(111), Cu(111) and Cu(100) surfaces was scrutinized by scanning tunneling microscopy as well as theoretical calculations. Detailed experimental evidence showed that whether the initially formed organometallic intermediate self-assembled or sparsely dispersed at surfaces essentially determined its subsequent reaction pathways. In specific, the assembled organometallic intermediates at full coverage underwent a single-barrier process to directly convert into the final coupling products while the sparsely dispersed ones at low coverage went through a double-barrier process via newly identified clover-shaped intermediates prior to their formation of the final coupling products. This demonstrates that the self-assembly strategy can efficiently steer surface reaction pathways and dynamics.

Several studies have been reported with focuses on the adsorption configurations or active sites of the reacting molecules self-assembled at surfaces.^[1-9] Very recently, we reported that the self-assembly of 4,4'-Bis(2,6-difluoropyridin-4-yl)-1,1':4',1''-terphenyl (BDFPTP) molecules could rigorously steer the regioselectivity of the dehydrocyclization reaction and suppress defluorinated coupling due to restricted docking orientations of the BDFPTP molecules prior to reaction commencement.^[10]

Substrate-induced confinement effect on surface reaction has been previously reported.^[11-14] However, the confinement effect caused by the mobile reacting molecules themselves has not been fully explored. Such an effect may be termed as self-confinement effect. A well-known phenomenon in solution chemistry^[15,16] is the so-called cage effect which states that the reacting molecules in solution are engaged by neighboring solvent molecules. Therefore, the diffusion probability for the reacting molecules out of the cage is drastically lowered, but the collision frequency of these molecules inside the cage greatly increases so that the average reaction rate becomes comparable with, if not higher than, its counterpart in gaseous phase. Surface molecular assembly strategy actually resembles such a cage effect by restricting the molecules in confined surface spacing

surrounded by themselves so that the assembling molecules dock to each other in specific ways to enhance their local collision probability and hence, their reaction rate inside the self-assembly may be remarkably enhanced. Meanwhile, other possible reactions that usually take place in solution chemistry may be suppressed because the docking manners of the reacting molecules may be completely different in solution and at surface. With such a concept in mind, we hereafter employ the surface assembly strategy to steer the reaction dynamics for Ullmann coupling of Br-containing molecules.

Ag(111) was chosen as the catalytic surface for the Ullmann coupling of 4-bromobiphenyl (denoted as BBP), C₆H₅C₆H₄Br. Ullmann coupling reaction is of great significance in constructing surface covalent nanostructures by using halogen-containing aromatic derivatives.^[17-20] Up to date two types of surface intermediates have been identified,^[13] depending on how the aromatic species are bonded to surface metal atoms: free-standing organometallic intermediates^[21-24] and surface-anchored aromatic species.^[25-29] The reaction processes were carefully monitored by scanning tunneling microscopy (STM) at various coverages, revealing that the Ullmann coupling reactions adopted different reaction pathways, as shown by the chemical equations in Figure 1a. Initially, the BBP molecules were deposited onto the Ag(111) surface at ~120 K and physically adsorbed on surface, correspondingly at coverage of 0.1 monolayer (ML, Figure 1b), 0.5 ML (Figure 1f) and 1 ML (Figure 1j). An individual BBP molecule is highlighted in the inset in Figure 1b which displays an uneven protrusion of the BBP molecule in the STM image, appearing like a tadpole. The bright endpoint protrusion is due to the Br atom in the molecule. In various clustered BBP aggregates (Figures. 1b, 1f and 1j), the molecules are held together via the halogen and weak hydrogen bond interactions.^[22,30,31]

When warmed up to RT and dwelt for a sufficient period of time (~30 minutes), all BBP molecules (~1.0 nm in length) converted into three-kernel-peanut-shaped features (~2.1 nm, Figure 1c). Many previous studies^[21-24] have shown that these features are ascribed to an Ag-coordinated organometallic intermediate (denoted as Ag-COI), C₆H₅C₆H₄AgC₆H₄C₆H₅, which is formed by two biphenyl moieties after Br detachment and one Ag adatom. The Ag-COIs sparsely distributed at 0.1 ML (Figure 1c) and formed a fishbone-like assembly structure at 1.0 ML (Figure 1k). At about 0.5 ML, both assembled (in islands) and unassembled Ag-COI co-existed (Figure 1g).

At 0.1 ML, however, a new intermediate was observed prior to the formation of the final coupling product (Figure 1b-e, Figure S1). The new intermediate, a 3-armed clover, was identified (Figure 1d), in which each arm was measured to be ~1.0 nm, being very close to the length of a biphenyl. An angle of 120° established between two neighboring arms in the clover intermediate (denoted as CI). Annealing the sample at 400 K for 5 minutes led to a large number of 3-armed CIs (Figure 1d), indicating that they were not accidentally formed by simple staying together of three biphenyl moieties. At this temperature with full coverage, some Ag-COIs directly converted into the p-

[*] Dr. X. Zhou, Dr. Y. Zhang, Dr. F. Cheng, Dr. Y. He, Dr. Q. Shen, Dr. J. Shang, Prof. K. Wu
BNLMS, College of Chemistry and Molecular Engineering, Peking University
Beijing 100871, China
E-mail: kaiwu@pku.edu.cn
Mr. C. Wang, Prof. W. Ji
Department of Physics, Renmin University of China, Beijing 100872, China.
E-mail: wji@ruc.edu.cn
Prof. X. Shao
Department of Chemical Physics, School of Chemistry and Materials Science, University of Science and Technology of China
Hefei 230026, China
E-mail: shaox@ustc.edu.cn
Prof. W. Chen, Prof. G. Xu
Department of Chemistry, National University of Singapore, Singapore 117543, Singapore.

[S] Supporting information for this article can be found under:
<http://dx.doi.org/>

COMMUNICATION

quaterphenyl (denoted as QP) product and other Ag-COIs remained intact, while no CIs were observed (Figure S2). A high-resolution STM image of the 3-armed CI is given in the inset in Figure 1d with the Ag(111) lattice structure superimposed as white grids, allowing determination of the topology of the CI at surface. Each arm of the CI deviated by about 8° against the $\langle 1\bar{1}0 \rangle$ lattice direction on Ag(111). This orientation was different

from that for the QP product which strictly oriented along the $\langle 1\bar{1}0 \rangle$ direction. Moreover, the inward ending of each biphenyl arm precisely pointed towards a lattice Ag atom in the substrate, indicating that the biphenyl was anchored to a surface Ag atom. Based on the experimental data, we therefore propose that each CI contains three biphenyls, $C_6H_5C_6H_4^*$.

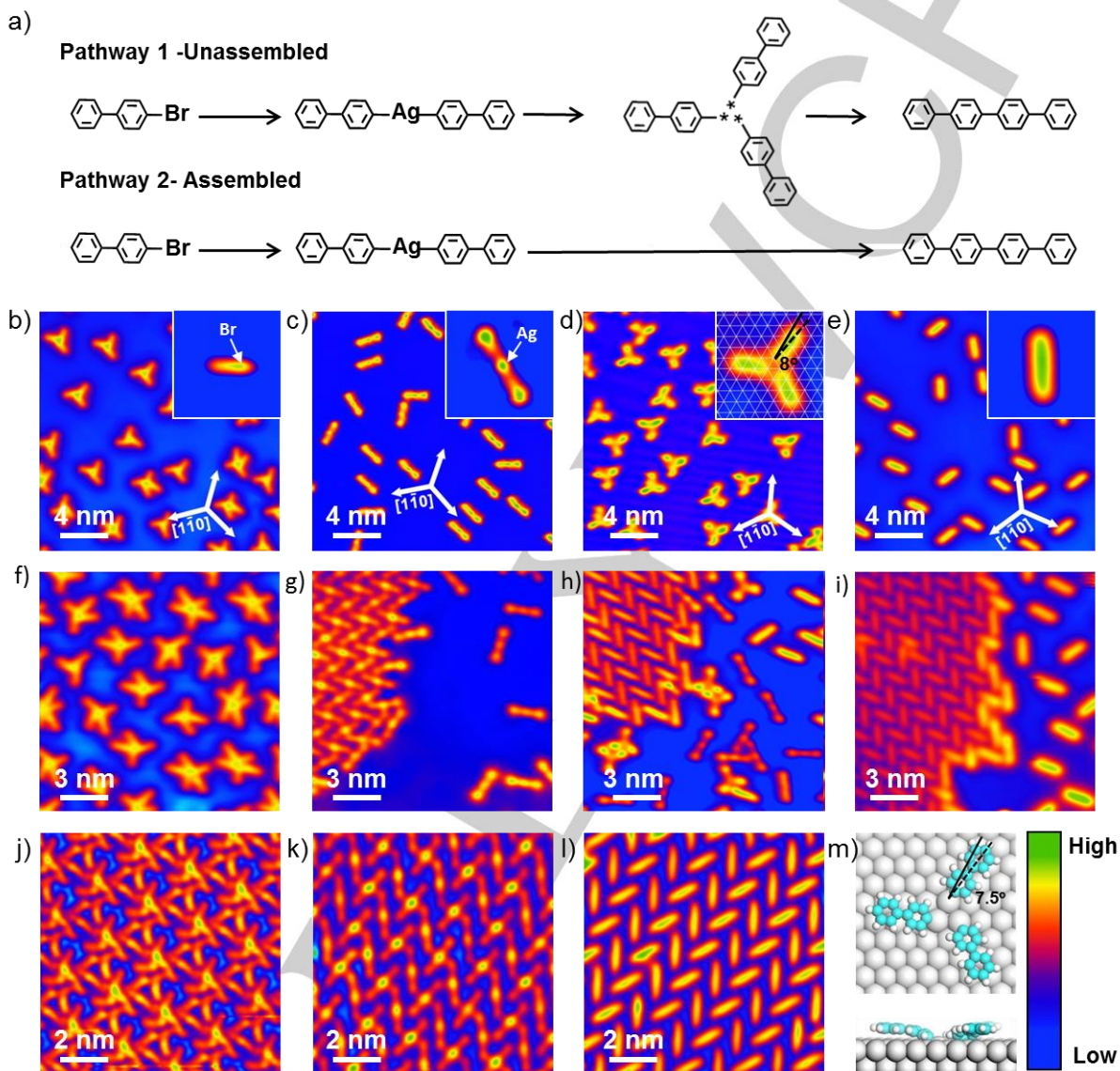


Figure 1. Self-assembly steered reaction pathways of the Ullmann coupling of BBP on Ag(111). (a) Chemical equations showing the pathways of the Ullmann coupling on Ag(111). (b)-(e) Four reaction steps of pathway 1 at 0.1 ML, involving BBP adsorption (120 K, b), formation of Ag-COI (300 K, c), CI (400 K, d) and QP (430 K, e). Insets in (b)-(e) are corresponding STM images of the individual BBP, Ag-COI, CI and QP. 2.5 nm \times 2.5 nm. (f)-(i) Four reaction steps at 0.5 ML, involving BBP (120 K, f), assembled Ag-COI island surrounded by unassembled Ag-COI (300 K, g), QP in the island out-skirted by CI (420 K, h), and the complete formation of QP (430 K, i). (j)-(l) Three reaction steps of pathway 2 at 1.0 ML, involving BBP (120 K, j), Ag-COI (300 K, k) and QP (420 K, l). (m) Top (upper part) and side (lower part) view of the theoretically optimized configuration of the CI on Ag(111). Color bar at the right side of (m) indicates the apparent height in the STM images.

To support the above assignment, DFT calculations were performed. The CI consisting of three biphenyls was optimized as a whole on Ag(111) to achieve its most favorable adsorption configuration where each arm deviated by about 7.5° from the $\langle 1\bar{1}0 \rangle$ direction (Figure 1m), in agreement with our STM result (8° , Figure 1d). The adsorption energy is -2.03 eV, about 0.40 eV

lower than that along the $\langle 11\bar{2} \rangle$ direction (-1.87 eV), as a comparison (Figure S3a). Three biphenyls species stayed together via their anchored Ag atoms which were slightly lifted upward by 0.5 Å (lower part in Figure 1m). A natural question then arises: why did the three biphenyls stick together to form a 3-armed clover? Our DFT calculations suggested that there was an

COMMUNICATION

energy gain of -0.99 eV when three biphenyls stayed together to form a cluster (Figure S3b). In addition, the calculated DOS of the CI depicted a bound state at -0.12 eV below the Fermi level if they adopted the configuration shown by the upper part in Figure 1m (also see Figure S3c and S3d). The DFT calculations therefore implied that these three biphenyls actually formed a clover-like organometallic complex,^[32] with three closely packed Ag atoms in the topmost layer of the substrate serving as the core of the complex. Similar Ag- or Cu-coordinated clusters stabilized by phenyl or phenyl derivatives have been previously proposed.^[33-35] Nevertheless, the CI could be fairly rationalized in terms of its energetics according to our DFT calculations. Eventually, most CIs turned into the final coupling products, QP, upon thermal treatment at 430 K for 5 minutes (Figure 1e).

With detailed descriptions and analyses of the 1 ML and 0.1 ML situations, dealing with the middle coverage (~0.5 ML) one is rather straightforward. At RT, the adsorbed BBP molecules (Figure 1f) would detach the Br atoms and self-assemble into densely packed Ag-COI islands surrounded by sparsely dispersed Ag-COIs (Figure 1g). The assembled Ag-COIs in the islands directly formed the QP products at 420 K (Figure 1h), while the surrounding Ag-COIs transformed into the CIs at the same temperature (Figure 1h). The CIs finally turned into the QP products at 430 K (Figure 1h). Therefore, the Ag-COIs in the compact islands behaved like those at 1 ML while the outshirting ones resembled those at ~0.1 ML, i.e. forming the CIs prior to the formation of the coupling products at a higher temperature. Again, assembly-steering of the reaction pathways was clearly demonstrated inside and outside the Ag-COI island.

To further confirm the ubiquity of assembly-steered reaction pathways for the Ullmann coupling reaction, Cu(111) and Cu(100) substrates were employed (Figure 2). At RT, similar Cu-coordinated organometallic intermediates (denoted as Cu-COIs), $C_6H_5C_6H_4CuC_6H_4C_6H_5$, were generated on Cu(111) (Figure 2a, d) and Cu(100) (Figure 2f, i). At 0.1 ML, the unassembled Cu-COIs were exclusively formed, orienting along $\langle 1\bar{1}0 \rangle$ direction on Cu(111) (Figure 2a) and $\langle 001 \rangle$ direction on Cu(100) (Figure 2f), respectively. Further warming up to 450 K led to the formation of the 3-armed CIs on Cu(111) with a C_{3v} symmetry (Figure 2b), very similar to that on Ag(111). However, 4-armed CIs with a C_{4v} symmetry were formed from Cu-COIs on Cu(100) at 480 K (Figure 2g). The neighboring arms in the 3-armed and 4-armed CIs formed an angle of 120° (inset in Figure 2b) and 90° (inset in Figure 2g), respectively, indicating that the biphenyl moieties were strongly dictated by the symmetry of the underlying substrate lattice. This can be feasibly understood because the Cu(111) and Cu(100) substrates possess a close-packed hexagonal and square surface lattice structure, respectively.

When the Cu-COIs self-assembled, however, the reaction pathway changed. The reaction process became quite simple that no CIs were formed, and Cu-COIs directly turned into the QP products at 460 K on Cu(111) (Figure 2e) and 470 K on Cu(100) (Figure 2j), respectively. The packing patterns of the coupling products appeared different, leading to the fishbone-like structure on Cu(111) (Figure 2e) and bricklike structure on Cu(100) (Figure 2j). According to our experimental observations described above, it is inevitable that the reaction pathways are steered by the self-assembly of the intermediates. The CIs finalize the Ullmann

coupling of BBP if the Cu-COIs sparsely disperse at surfaces, while direct Ullmann coupling takes place if the Cu-COIs self-assemble at surfaces. To understand this phenomenon, it is necessary to scrutinize the reaction dynamics.

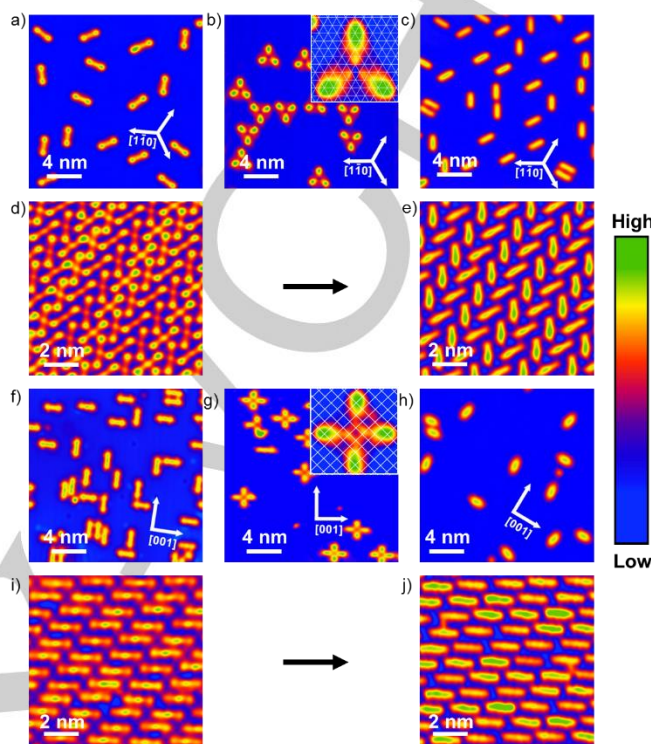


Figure 2. Self-assembly steered reaction pathways of the Ullmann coupling from Cu-COI to QP on Cu(111) and Cu(100). (a)-(c) Reaction process of pathway 1 on Cu(111), involving formation of (a) Cu-COI at 300 K, (b) CI at 450 K, and (c) QP at 480 K. Inset in (b) is high resolution image of the 3-armed CI with overlaid surface lattice of the Cu(111) substrate. $2.5 \text{ nm} \times 2.5 \text{ nm}$. (d),(e) Reaction process of pathway 2 on Cu(111), involving formation of (d) Cu-COI at 300 K and (e) QP at 460 K. (f)-(h), Reaction process of pathway 1 on Cu(100), involving formation of (f) Cu-COI at 300 K, (g) CI at 480 K, and (h) QP at 500 K. Inset in (g) is high resolution image of the 4-armed CI with the overlaid surface lattice of the Cu(100) substrate. $2.7 \text{ nm} \times 2.7 \text{ nm}$. (i), (j) Reaction process of pathway 2 on Cu(100), involving formation of (i) Cu-COI at 300 K and (j) QP at 470 K. Color bar at the right side indicates the apparent height in the STM images.

Due to the uncertainty and complexity of the transition state species after Ag-COI dissociation, DFT calculations did not provide convincing results about the reaction dynamics. We therefore experimentally measured the reaction energy barriers by treating the Ag-COI as reacting reagents, which should help explore the working principle of the self-assembly strategy.

According to Arrhenius equation, the rate constant can be expressed as:

$$k = Ae^{-\frac{E}{RT}}, \quad (1)$$

where k is the rate constant, A is the pre-exponential factor, E is the energy barrier and R is the universal gas constant, T is the reaction temperature. In order to experimentally elucidate the energy barriers, the equation is rearranged as,

$$\ln k = \ln A - \frac{E}{RT}. \quad (2)$$

COMMUNICATION

Therefore, a plot of $\ln k$ versus $1/T$ would yield the slope of the linear relationship, $-E/R$, and E for each step. Similar method has been applied to measure the migration barrier for diffusion.^[36,37] The rate constant k can be determined by monitoring the unconverted molecule ratio of before and after heating the sample in time t (SI Experimental methods: Dynamics measurements, Figure S4). The experimental plots of $\ln k$ versus $1/T$ are given in the inset of Figure 3.

According to Figure 3, the first energy barrier in pathway 1, E_{u1} (u stands for unassembled), for the conversion of Ag-COI into CI was 0.88 ± 0.17 eV, and the second one, E_{u2} , for the conversion of CI into QP, 1.23 ± 0.32 eV. In pathway 2, the energy barrier, E_a (a stands for assembled), for the direct conversion of Ag-COI into QP was deduced to be 1.10 ± 0.23 eV. Based on the intercepts of the plots, the pre-exponential factor, A , was calculated: $A_{u1} = 2 \times 10^8$ s⁻¹, $A_{u2} = 5 \times 10^8$ s⁻¹ and $A_a = 2 \times 10^{11}$ s⁻¹.

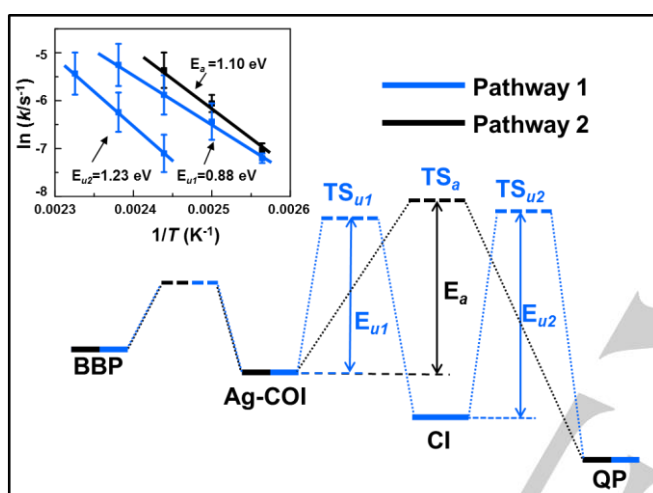


Figure 3. Experimentally measured potential energy diagram for the Ullmann coupling reactions in different pathways. In pathway 1, the CI appears prior to the QP formation, while in pathway 2, the coupling product QP is directly generated from organometallic intermediate, resulting in self-assembly steered reaction pathways.

A general picture for the formation of the coupling products has been achieved by theoretical calculations that surface-bonded aryl species diffuse on surface, collide and combine together at a suitable temperature.^[38,39] Our experimental identification of the CIs indicated that the surface-anchored aryl species retained at surfaces after dissociation of the Ag-COIs. A possible scenario for both pathways is that after the dissociation of the Ag-COIs, the formed surface-anchored aryl species diffuse at surface and encounter others in two possible manners. When sparsely dispersed, the Ag-COIs can diffuse freely at surface, and the energy barrier for the formation of the CIs is 0.22 eV lower than that for direct generation of QP, which makes the rate constant of the former is $\sim 10^3$ times higher than the latter at 400 K. That is the main reason why Ag-COIs choose pathway 1. However, when the Ag-COIs self-assemble, their diffusion and rotation are remarkably restricted in the self-assembly acting like a cage. In consideration of the specific structure of the Ag-COI assembly, once formed, the aryl species tend to collide head to head, and the generation of the CIs need to break the assembly structure. Both indicate that the pre-exponential factor for direct QP

formation is much higher than that for the CI generation. Thus the Ag-COIs adopt pathway 2. Since no CIs are observed when the Ag-COIs are assembled, the ratio of the pre-exponential factors or rate constants could not be experimentally measured. Nevertheless, the self-assembly strategy does exert a strong influence in the pre-exponential factors for both reaction pathways.

Moreover, the energy barrier, E_{u2} (1.23 eV), was about 0.13 eV higher than E_a (1.10 eV), leading to that the coupling reaction to the final product from the sparsely dispersed Ag-COIs takes place at a higher temperature, i.e. 430 K, than that, i.e. 410 K, from the assembled Ag-COIs at full coverage.

To conclude, the above experimentally measured reaction energetics and dynamics for the initially formed Ag-COIs in different existence states, either assembled or unassembled, at surfaces can well explain reaction pathways steered by the surface assembly strategy. In particular, the activation temperatures for the organometallic intermediates to QP reactions on all three surfaces studied, namely, Ag(111), Cu(111) and Cu(100), were at least 10 ~ 30 K lower starting from the unassembled Ag-COIs than that from the assembled ones. Our experimental results clearly demonstrate that the surface reaction pathways can be efficiently steered by the self-assembly strategy which may be further employed to tweak reactions in surface chemistry.

Acknowledgements

This work was jointly supported by NSFC (91527303, 21333001, 21261130090) and MOST (2017YFA0204702, 2013CB933400), China. XS is grateful for the financial support of the Thousand Talent Program for Young Outstanding Scientists of the Chinese government.

Keywords: Self-assembly Strategy • Surface Reaction Dynamics • Ullmann coupling • Scanning Tunnelling Microscopy

- [1] Y.-T. Shen, L. Guan, X.-Y. Zhu, Q.-D. Zeng, C. Wang, *J. Am. Chem. Soc.* **2009**, *131*, 6174.
- [2] M. Kim, J. N. Hohman, Y. Cao, K. N. Houk, H. Ma, A. K.-Y. Jen, P. S. Weiss, *Science* **2011**, *331*, 1312.
- [3] S. A. Claridge, W.-S. Liao, J. C. Thomas, Y. Zhao, H. H. Cao, S. Cheunkar, A. C. Serino, A. M. Andrews, P. S. Weiss, *Chem. Soc. Rev.* **2013**, *42*, 2725.
- [4] H.-Y. Gao, D. Zhong, H. Moenig, H. Wagner, P.-A. Held, A. Timmer, A. Studer, H. Fuchs, *J. Phys. Chem. C* **2014**, *118*, 6272.
- [5] L.-Z. Wu, B. Chen, Z.-J. Li, C.-H. Tung, *Acc. Chem. Res.* **2014**, *47*, 2177.
- [6] F. Sedona, M. Di Marino, D. Forrer, A. Vittadini, M. Casarin, A. Cossaro, L. Floreano, A. Verdini, M. Sambi, *Nat. Mater.* **2012**, *11*, 970.
- [7] L. Zhang, M. Lepper, M. Stark, D. Lungerich, N. Jux, W. Hieringer, H.-P. Steinruck, H. Marbach, *Phys. Chem. Chem. Phys.* **2015**, *17*, 13066.
- [8] D. Teschner, G. Novell-Leruth, R. Farra, A. Knop-Gericke, R. Schlögl, L. Szentmiklósi, M. G. Hevia, H. Soerijanto, R. Schomäcker, J. Pérez-Ramírez, N. López, *Nat. Chem.* **2012**, *4*, 739.
- [9] O. R. Inderwildi, D. Lebiez, J. Warnatz, *Phys. Chem. Chem. Phys.* **2005**, *7*, 2552.

COMMUNICATION

- [10] Q. Chen, J. R. Cramer, J. Liu, X. Jin, P. Liao, X. Shao, K. V. Gothelf, K. Wu, *Angew. Chem.* **2017**, *129*, 5108-5112.
- [11] Q. Fan, J. Dai, T. Wang, J. Kuttner, G. Hilt, J. M. Gottfried, J. Zhu, *ACS Nano* **2016**, *10*, 3747-3754.
- [12] D. Zhong, J.-H. Franke, S. K. Podiyanchari, T. Blömker, H. Zhang, G. Kehr, G. Erker, H. Fuchs, L. Chi, *Science* **2011**, *334*, 213-216.
- [13] Q. Fan, J. M. Gottfried, J. Zhu, *Acc. Chem. Res.* **2015**, *48*, 2484.
- [14] J. A. Lipton-Duffin, O. Ivashenko, D. F. Perepichka, F. Rosei, *Small* **2009**, *5*, 592-597.
- [15] J. Franck, E. Rabinowitsch, *Trans. Faraday Soc.* **1934**, *30*, 120.
- [16] D. A. Braden, E. E. Parrack, D. R. Tyler, *Coord. Chem. Rev.*, **2001**, 211, 279.
- [17] L. Lafferentz, F. Ample, H. Yu, S. Hecht, C. Joachim, L. Grill, *Science* **2009**, *323*, 1193.
- [18] J. Cai, P. Ruffieux, R. Jaafar, M. Bieri, T. Braun, S. Blankenburg, M. Muoth, A. P. Seitsonen, M. Saleh, X. Feng, K. Mullen, R. Fasel, *Nature* **2010**, *466*, 470.
- [19] H. Zhang, H. Lin, K. Sun, L. Chen, Y. Zagranyski, N. Aghdassi, S. Duhm, Q. Li, D. Zhong, Y. Li, K. Müllen, H. Fuchs, L. Chi, *J. Am. Chem. Soc.* **2015**, *137*, 4022.
- [20] A. Basagni, F. Sedona, C. A. Pignedoli, M. Cattelan, L. Nicolas, M. Casarin, M. Sambri, *J. Am. Chem. Soc.* **2015**, *137*, 1802.
- [21] R. Gutzler, H. Walch, G. Eder, S. Kloft, W. M. Heckl, M. Lackinger, *Chem. Commun.* **2009**, 4456.
- [22] J. Park, K. Y. Kim, K.-H. Chung, J. K. Yoon, H. Kim, S. Han, S.-J. Kahng, *J. Phys. Chem. C* **2011**, *115*, 14834.
- [23] W. Wang, X. Shi, S. Wang, M. A. Van Hove, N. Lin, *J. Am. Chem. Soc.* **2011**, *133*, 13264.
- [24] E. A. Lewis, C. J. Murphy, M. L. Liriano, E. C. H. Sykes, *Chem. Commun.* **2014**, *50*, 1006.
- [25] M. Xi, B. E. Bent, *J. Am. Chem. Soc.* **1993**, *115*, 7426.
- [26] M. Bieri, M.-T. Nguyen, O. Gröning, J. Cai, M. Treier, K. Ait-Mansour, P. Ruffieux, C. A. Pignedoli, D. Passerone, M. Kastler, K. Müllen, R. Fasel, *J. Am. Chem. Soc.* **2010**, *132*, 16669.
- [27] P. S. Weiss, M. M. Kamna, T. M. Graham, S. J. Stranick, *Langmuir* **1998**, *14*, 1284.
- [28] S.-W. Hla, L. Bartels, G. Meyer, K.-H. Rieder, *Phys. Rev. Lett.* **2000**, *85*, 2777.
- [29] E. A. Lewis, C. J. Murphy, A. Pronschinske, M. L. Liriano, E. C. H. Sykes, *Chem. Commun.* **2014**, *50*, 10035.
- [30] G. R. Desiraju, R. Parthasarathy, *J. Am. Chem. Soc.* **1989**, *111*, 8725.
- [31] J. Shang, Y. Wang, M. Chen, J. Dai, X. Zhou, J. Kuttner, G. Hilt, X. Shao, J. M. Gottfried, K. Wu, *Nat. Chem.* **2015**, *7*, 389.
- [32] G. A. Somorjai, *Pure and Applied Chemistry* **1988**, *60*, 1499.
- [33] D. Nobel, G. van Koten, A. L. Spek, *Angew. Chem. Int. Ed.* **1989**, *28*, 208.
- [34] P. Belanzoni, M. Rosi, A. Sgamellotti, E. J. Baerends, C. Floriani, *Chem. Phys. Lett.* **1996**, *257*, 41.
- [35] M. Stollenz, F. Meyer, *Organometallics* **2012**, *31*, 7708.
- [36] H. Marbach, H. P. Steinrück, *Chem. Commun.* **2014**, *50*, 9034.
- [37] S. Ditze, M. Stark, M. Drost, F. Buchner, H.-P. Steinrück, H. Marbach, *Angew. Chem. Int. Ed.* **2012**, *51*, 10898.
- [38] J. Björk, F. Hanke, S. Stafström, *J. Am. Chem. Soc.* **2013**, *135*, 5768.
- [39] M.-T. Nguyen, C. A. Pignedoli, D. Passerone, *Phys. Chem. Chem. Phys.* **2011**, *13*, 154.

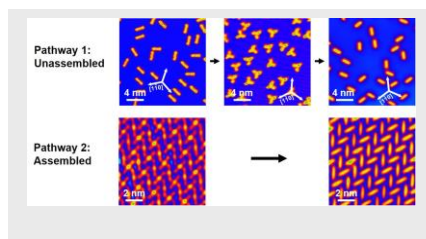
COMMUNICATION

Entry for the Table of Contents (Please choose one layout)

Layout 1:

COMMUNICATION

Self-assembly Steered Surface Reaction Dynamics: During the Ullmann coupling of 4-bromobiphenyl on Ag and Cu surfaces, self-assembled organometallic intermediates directly form the final product while the unassembled ones undergo via formation of the clover intermediates prior to formation of the final product, demonstrating the self-assembly strategy can efficiently steer the surface reaction pathways.



Xiong Zhou, Chenguang Wang, Yajie Zhang, Fang Cheng, Yang He, Qian Shen, Jian Shang, Jianlong Li, Xiang Shao*, Wei Ji*, Wei Chen, Guoqin Xu, Kai Wu*

Page No. – Page No.

Steering Surface Reaction Dynamics with Self-Assembly Strategy